applied sciences

MDPI

Article

Multi-Stage Topology Optimization for Structural Redesign of Railway Motor Bogie Frames

Alessio Cascino *, Enrico Meli and Andrea Rindi

Department of Industrial Engineering, University of Florence, 50139 Florence, Italy
* Correspondence: alessio.cascino@unifi.it

Abstract

This study presents a comprehensive structural optimization workflow for a railway motor bogie frame, aimed at developing an innovative and lightweight design compliant with the reference European standards. The methodology integrates a two-stage topology optimization process, supported by an extensive numerical simulation campaign and a dedicated sensitivity analysis to identify the most critical load scenarios. In the first optimization stage, a global evaluation of the frame performance revealed that increasing the number of optimization parameters leads to a rise of approximately 50% in solver iterations. Symmetry constraints proved essential for simplifying both the optimization and the subsequent geometric reconstruction. The minimum feasible feature dimension strongly affected the final solution, modifying the material distribution and enabling a mass reduction of about 18%. The second optimization stage, focused on the cross beams, highlighted the relevance of manufacturing constraints in guiding the solver toward practical configurations. Static and fatigue assessments confirmed stress distributions consistent with the original frame, providing designers with a reliable basis for future material upgrades. Finally, the dynamic analysis showed a first natural frequency above 60 Hz, with variations in the first eigenvalue within 1% and preservation of the local flexural mode shape, ensuring full compatibility with the original frame interfaces and enabling seamless replacement with the optimized configuration.

Keywords: topology optimization; lightweight design; digital twin; finite element model; sensitivity analysis; railway vehicle design; railway dynamics

Academic Editors: Ján Dižo, Alyona Lovska and Miroslav Blatnický

Received: 10 December 2025
Revised: 14 January 2026
Accepted: 15 January 2026
Published: 18 January 2026

1. Introduction

In modern railway engineering, the demand for components that combine low structural mass with high mechanical robustness has become increasingly relevant, as weight reduction contributes to lower energy consumption, reduced track loading, and enhanced dynamic behavior. Despite the growing interest in advanced optimization strategies, topology optimization is still not formally integrated into the European design standards governing railway bogies, which continue to rely mainly on traditional analytical and numerical verification procedures. This limitation slows the adoption of more innovative design approaches, even though their benefits have been widely demonstrated in other engineering sectors. Moreover, the development of lightweight structural solutions for assemblies as complex as motor bogie frames must remain fully compliant with stringent safety and performance requirements, making the introduction of new methodologies particularly challenging. In this context, this study addresses this gap by proposing an integrated optimization-and-validation workflow for the structural redesign of a railway

motor bogie frame, demonstrating how a carefully parameterized and standard-oriented process can lead to an innovative yet compliant structural solution. Topology optimization has become a consolidated tool in the automotive sector, where it is routinely employed during the conceptual development of body and chassis structures to reduce mass while ensuring adequate stiffness and crashworthiness. Numerous investigations have reported substantial improvements in structural efficiency for both metallic and composite vehicle components, confirming the effectiveness of optimization-driven design routes in real engineering applications [1–6]. Parallel efforts have also focused on refining manufacturing processes through optimization methodologies, demonstrating that production constraints can be effectively embedded to achieve geometries that balance performance and manufacturability [7–10]. A complementary research direction concerns the integration of optimization methods with additive manufacturing (AM). In fields such as turbomachinery, this combination has enabled the realization of lightweight components with efficient load paths and geometries beyond the limits of conventional fabrication, demonstrating meaningful gains in structural performance and design flexibility [11–17]. Within the railway engineering field, the application of structural optimization is still limited, despite increasing interest in recent years. Railway vehicles are composed of complex multi-component assemblies, where each structural element must simultaneously satisfy stringent requirements for strength, stiffness, fatigue resistance, and dynamic performance under highly variable and coupled load scenarios. With reference to the railway bogie frame, research activities are significantly fewer, mainly due to the higher complexity of the application and the fact that optimization-based design has not yet become an established practice in this field. The bogie frame of a tilting train operating on the Korean railway network was redesigned through an optimization approach based on a micro genetic algorithm, demonstrating the potential of algorithm-driven design for improving performance and efficiency [18]. Similarly, a targeted structural optimization study addressing the bogie frame and bolster of a freight wagon is presented in [19], aiming primarily at reducing the overall mass of the assembly. The authors applied a topology optimization strategy using the SIMP method to enhance structural stiffness while minimizing material usage. The incorporation of manufacturing constraints and integration with multibody simulation environments have been investigated in [20]. More broadly, a range of optimization strategies has been explored in [21–24], assessing the effects of manufacturing limitations and considering both metallic and composite material systems. The literature also highlights the importance of railway bogie frame life prediction. Comparable modelling strategies have been extended to several bogie frame typologies, confirming the relevance of coupled dynamic analyses for capturing realistic load scenarios [25–27]. In parallel, durability-oriented studies have examined welded A-frame structures used in heavy-duty mining vehicles, combining fatigue assessment with optimization procedures to enhance service life [28]. Additional contributions include experimental fatigue investigations performed on metro bogie frames [29,30] and comprehensive stress and acceleration campaigns carried out on diesel multiple-unit (DMU) bogie frames to diagnose the mechanisms responsible for fatigue crack initiation [31]. The scientific literature also highlights a growing interest in the application of structural optimization techniques to railway car bodies, both for conventional metallic structures and for more advanced composite solutions [32–34]. Recent studies have demonstrated how optimization-based methodologies can support weight reduction, stiffness enhancement, and improved load-path efficiency in large welded assemblies, while maintaining compliance with the stringent safety and durability requirements of railway applications [35,36]. These approaches have been employed not only for static strength assessment but also in the refinement of dynamic behavior [37], where modal performance, vibration attenuation, and fatigue resistance play a crucial role in

the overall structural response of the vehicle. This expanding research trend confirms the potential of advanced optimization tools to support the next generation of lightweight, high-performance railway structures. Despite the growing interest in lightweight and high-performance railway structures of different types, no established methodology currently exists for applying multi-stage topology optimization to motor bogie frames while ensuring full compliance with structural, fatigue and modal requirements. This work fills this gap by introducing a complete optimization and validation workflow for the redesign of a railway motor bogie frame.

2. Methodology and Benchmark Description

This section outlines the research methodology and provides a comprehensive description of the benchmark case study. Specifically, a detailed technical characterization of the motor bogie frame is presented, followed by a formal definition of the optimization framework, including its primary objectives, constraints, and algorithmic settings.

2.1. Methodology

The present research activity was conceived with the objective of advancing the design of one of the most mechanically demanding components of a railway vehicle: the bogie frame. With this aim, a comprehensive structural-optimization procedure was developed, ensuring full compliance with the European standards governing the mechanical assessment of bogie structures. The methodological framework was designed to integrate high-fidelity numerical modelling, standardized mechanical verification, and iterative optimization strategies, ultimately enabling the generation of an innovative bogie-frame concept. The workflow, described in detail in the following points, is articulated into several key stages that collectively support the development, evaluation, and refinement of the optimized design:

(1) A high-fidelity finite element (FE) model of the bogie frame was developed, including all equipment supports and the fundamental load interfaces required to properly reproduce the interactions with adjacent and interconnected subsystems;
(2) A complete mechanical assessment was performed, covering both static and fatigue verification in accordance with the applicable European standards. This step was followed by an extensive sensitivity analysis aimed at improving the efficiency and robustness of the computational procedure;
(3) A first topology optimization analysis was conducted on the entire design volume available for the bogie frame. A comprehensive numerical testing campaign was carried out to identify the optimal optimization settings capable of delivering results aligned with the project objectives;
(4) An intermediate performance assessment of the newly generated bogie-frame geometry was executed according to the reference European standard, allowing the early identification of potential critical issues;
(5) A second optimization cycle was then performed, this time targeting the redesign of the transversal beams, with the dual aim of improving both their mechanical performance and their geometric characteristics from a design-for-manufacturing perspective;
(6) Finally, a complete evaluation of the performance of the optimized geometry was conducted to validate the effectiveness of the proposed design.

This methodology is intended to address the existing gap whereby structural-topological optimization workflows often remain ineffective or scarcely applicable when dealing with highly complex components such as the bogie frame. The proposed approach provides an optimization process that is fully compliant with European standards while remaining streamlined, computationally efficient, and closely aligned with design-for-

manufacturing principles. By integrating high-fidelity modelling, standardized mechanical verification, and iterative refinement within a unified framework, the methodology enables the practical and reliable development of innovative bogie-frame geometries.

2.2. The Railway Motor Bogie Frame

The vehicle hosting the bogie frame, although not investigated in its entirety within the present study, would require a complete structural assessment in accordance with EN 12663-1 [38] and EN 15663 [39]. The vehicle was equipped with two different bogie configurations: trailer bogie frames and motor bogie frames. Considering the more demanding load paths, the presence of traction equipment, and the higher mechanical stress levels typically acting on powered assemblies, the investigation presented in this work focused on the most critical type: the motor bogie frame. Accordingly, the optimization methodology was specifically applied to this powered configuration, which was subsequently redesigned and structurally enhanced. The motor bogie frame under study is a robust steel structure [40], engineered to provide the strength, durability, and resilience required to endure the demanding operational conditions of a modern tram system. Its fabrication relies on precision welding techniques that ensure uniform and continuous joints between the structural components. Nonetheless, despite the accuracy of the manufacturing process, welded connections remain critical features, particularly with respect to fatigue-related issues arising under complex loading scenarios. Structurally, the frame consists of two longitudinal beams, two cross-members, and several accessory structural elements, all arranged to ensure an efficient distribution of loads throughout the assembly. This layout not only contributes to the overall stability of the bogie but also plays a key role in the safety and performance of the entire vehicle. The original configuration is made of structural steel and fully assembled through welded joints, as previously described. The central sections of the longitudinal beams host the interfaces for the secondary suspension, while the opposite ends accommodate the supports for the traction motor and the braking system. The attachment points for the two traction rods are instead located on the cross-members. A complete view of the original bogie-frame architecture is provided in Figure 1.

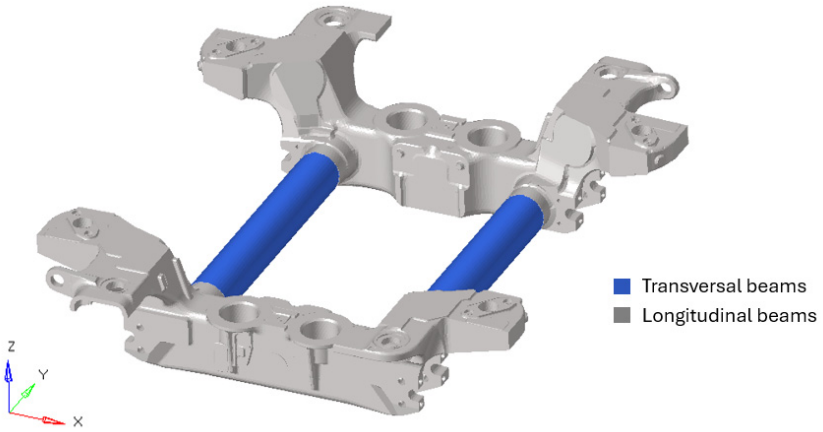

Figure 1. View of the original tram bogie frame's geometry.

Before detailing the meshing strategy and the specific modelling choices adopted, it is important to underline that the development of a high-fidelity finite element model is essential to realistically reproduce the operational behavior of the bogie frame. Achieving such a level of physical representativeness requires not only an accurate geometric reconstruction, but also a thorough understanding of the role and mechanical function of each modelling element introduced into the numerical model. Only through this comprehensive

approach can the FE model reliably capture the real load paths, stiffness distribution, and interaction mechanisms that characterize the in-service conditions of the bogie system. Figure 2 presents the finite element representation of the tested motor bogie frame. The model was constructed to capture the principal structural behavior of the assembly, using a combination of 0D, 1D, and 3D elements selected according to the mechanical role of each component. Owing to the substantial thicknesses and the markedly three-dimensional nature of the frame geometry, a shell-based formulation (QUAD elements) was deemed inadequate to reproduce the real stiffness distribution. For this reason, all primary structural members, including the longitudinal beams, the cross-members, and the various auxiliary brackets, were discretized using second-order tetrahedral elements (TETRA10), with the mesh density adjusted locally to ensure an appropriate level of refinement across the different regions of the bogie. The model contains more than 2 million nodes and more than 1.7 million elements. The connections between the supports and the frame were implemented through bonded (freeze) contact definitions. This modelling choice ensures a linear response while correctly transferring forces and moments across the interfaces. The bonded formulation enforces zero relative displacement between the involved surfaces, preserving the original gap and suppressing any sliding behavior. Such an approach offers a good compromise between numerical accuracy and modelling efficiency, while also simplifying subsequent modifications: each component can be updated independently as long as the contact interfaces are preserved, facilitating parametric variations and repeated numerical testing. The application of external loads was handled using a combination of concentrated forces, surface pressures, and RBE3 elements, depending on the loading condition and the area of application. The use of RBE3 elements was particularly advantageous, as these entities allow forces and moments to be distributed among several nodes without altering the stiffness of the model. The wheelsets were represented through one-dimensional elements, specifically a sequence of beam elements with cross-sectional and inertial properties consistent with the real components. This strategy preserved the correct mass distribution and bending behavior without resorting to more computationally expensive solid modelling. The primary suspension was likewise modelled using 1D elements following the same modelling philosophy. Reproducing this subsystem accurately was essential to avoid introducing artificially rigid constraints that could lead to unrealistic stress concentrations. For all analyzed load cases, the global boundary conditions were defined using an isostatic scheme. The constraint points were applied at the locations corresponding to the four wheels, situated at the ends of each axle, thereby ensuring a stable yet non-redundant support configuration.

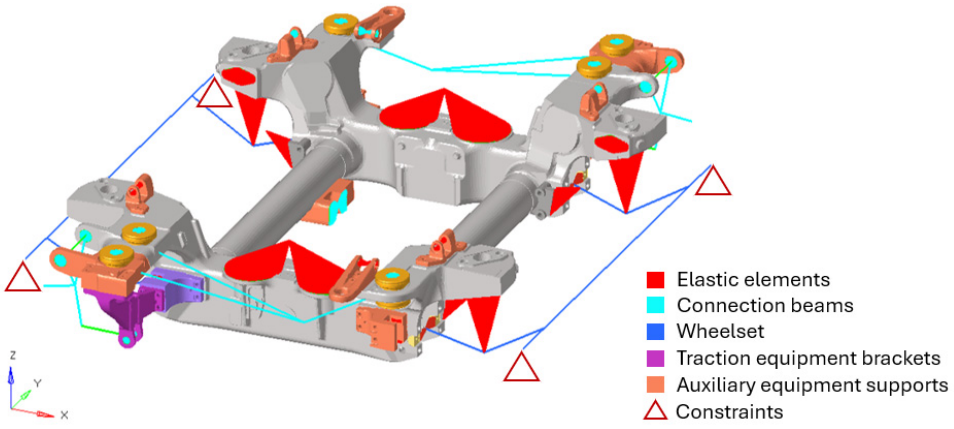

Figure 2. High-fidelity FE model of the motor bogie frame.

2.3. Topological Optimization Model and Settings

The topology optimization performed on the tram motor bogie frame was conceived with the aim of generating a redesigned structural layout capable of accommodating manufacturing solutions alternative to conventional welded assemblies. The optimization routine employed in this study relied on a gradient-based algorithm [41], which enabled an efficient exploration of the design space under multiple loading conditions, derived by sensitivity analysis described in the next section. The optimization target was defined as the reduction of the global weighted compliance [42–44], computed by combining the contributions associated with all the considered load cases. In this context, compliance, expressed as the total strain energy stored in the structure, provides a useful indicator of the component's deformation response. A lower compliance corresponds to a stiffer behavior, while higher values indicate greater flexibility under external loads. By framing the redesign problem in terms of minimizing the compliance, it was possible to drive the algorithm towards configurations characterized by improved stiffness efficiency and enhanced structural performance. Before initiating the optimization routine, the finite element model was reformulated to meet the requirements of the adopted methodology. The design domain, i.e., the portion of material allowed to evolve during the optimization, was enlarged to provide the solver with sufficient freedom to explore alternative structural configurations. Conversely, all regions involved in mechanical interfaces, mounting points for auxiliary equipment, and load-application areas were assigned to a fixed domain, called the non-design domain, and therefore excluded from modification. The optimization was constrained through a mass-fraction limit, defined as the ratio between the mass of the optimized layout and the initial mass of the design space. In accordance with common practice for this type of procedure, the threshold was set to 40%. The workflow, as explained in the previous section, consisted of two distinct optimization stages. In the first stage, the entire frame was treated as the design space, allowing the algorithm to distribute material freely across the whole bogie structure. This configuration is illustrated in Figure 3a, where the enlarged volume available to the solver is highlighted in green. This step was intended to identify the global load-carrying trends and to provide a preliminary estimate of the most structurally efficient regions. In this phase, the manufacturing constraints were also introduced, allowing an early assessment of the producibility of the geometries generated by the solver. Evaluating these constraints required a broad set of iterative simulations and represented the most demanding part of the numerical campaign, as each optimization condition had to be tested to quantify its influence on the structural response and to identify the most effective combination of parameters. The second stage focused instead on a refined redesign of the transversal beams. After the first optimization step, the frame had already undergone an initial topological innovation, and the results were used to define a new, more localized design domain. As shown in Figure 3b, the only regions subjected to the subsequent optimization loop are depicted in red. This selective approach allowed the algorithm to concentrate exclusively on the cross-member structures, with the aim of enhancing their performance while preserving manufacturability constraints, applied under different conditions.

The numerical optimization campaign conducted in this study involved an extensive sequence of tests, carried out by systematically varying the available design parameters and their mutual combinations. All reference configurations are summarized in Table 1, which reports the seven representative optimization setups selected among the numerous simulations performed. Each configuration is associated with a unique ID, allowing the corresponding optimization strategy to be easily traced and referenced in the presentation of results provided in the following sections. Optimization cases from ID01 to ID05 refer to simulations performed on the entire bogie frame, whereas ID06 and ID07 correspond to the

local optimization study, restricted to the transverse beams. The table also details, column by column, the specific parameter settings adopted in each iteration, thereby illustrating how the optimization strategy evolved throughout the research activity.

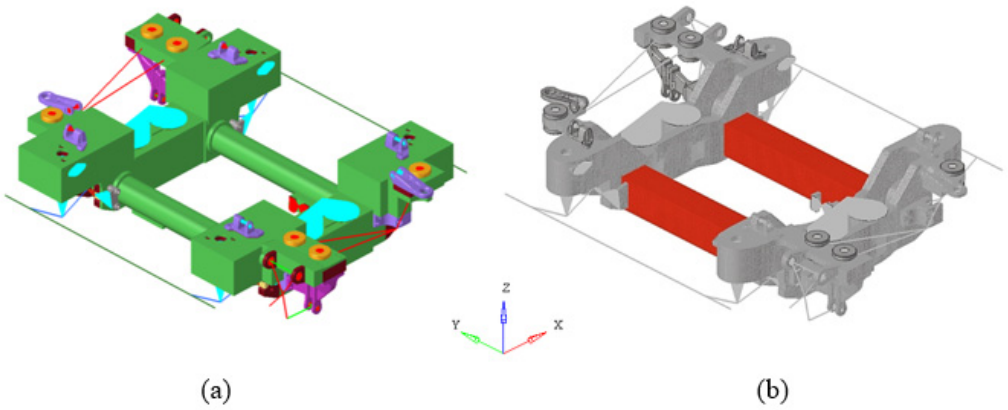

Figure 3. Motor bogie frame set for topological optimization defining design and non-design space: (**a**) first global optimization stage, (**b**) second local optimization stage.

Table 1. Numerical campaign of structural optimization: summary of settings.

Setting Name	Setting Description	Global Optimization				Local Optimization		
		ID01	ID02	ID03	ID04	ID05	ID06	ID07
Optimization objective	Weighted compliance minimization	yes	yes	yes	yes	yes	yes	yes
Optimization constraint	Mass fraction lower than a reference value	<0.4	<0.4	<0.4	<0.4	<0.4	<0.3	<0.3
Stress constraint	Calculated stress lower than a reference value	\	<300 MPa	<300 MPa	<300 MPa	<240 MPa	<240 MPa	<240 MPa
Geometrical pattern	Symmetry respect to a plane	\	plane xz	plane xz	plane xz	plane xz	plane xz	plane xz
Minimum feasible feature dimension	The minimum dimension acceptable for elements	\	25 mm	20 mm	15 mm	15 mm	15 mm	15 mm
Extraction direction	Removing material along reference direction	\	\	*y* axis	*y* axis	*y* axis	\	*y* axis

As previously outlined, the optimization procedure was governed by a mass-fraction constraint, defined as the ratio between the optimized mass and the initial mass of the design domain. For the global optimization phase, this ratio was limited to 40%, a threshold commonly adopted in topology optimization studies, while for the second, localized stage it was further reduced to approximately 30% to encourage a more refined redistribution of material. To prevent the solver from converging toward asymmetric layouts driven by unilateral loading conditions, a geometrical symmetry constraint was enforced through the "Geometrical pattern" option, imposing symmetry with respect to the mid-plane orthogonal to the y-axis. This ensured consistent material distribution across the structural halves despite the inherently unbalanced load application. The parameter controlling the minimum feasible feature dimension was initially set to 25 mm, then progressively reduced by about 40% as confidence in the emergent structural patterns increased. This setting regulated the minimum characteristic length scale permitted during the optimization, guaranteeing an adequate geometric resolution without generating unrealistically fine features.

The principal manufacturing constraint was the extraction direction, which compelled the material removal to occur along a predefined axis. This constraint effectively emulated the demolding process, ensuring that the resulting topology remained "open" either upward or downward depending on the selected direction, thus remaining compatible with potential forming or casting operations. Finally, a static stress constraint was introduced to avoid excessive thinning or elimination of material in regions where high stress concentrations could arise, thereby preserving structural integrity while allowing the algorithm to explore lighter, more efficient configurations.

3. Results and Discussion

This section presents and discusses the definition of the operational load scenarios, followed by the findings of the sensitivity analysis related to them. Subsequently, the outcomes of the topology optimization process are detailed, culminating in the presentation of the innovative motor bogie frame design and a discussion of its structural performance.

3.1. Load Scenario and Sensitivity Analysis

The structural evaluation of the metro motor bogie frame was performed by applying the loading scenarios defined in EN 13749:2021 [45]. Following the indications of the standard, twenty distinct conditions were simulated, encompassing both operational static loads and those required for fatigue verification. Each scenario incorporates several simultaneous load components acting on different regions of the bogie frame. In order to maintain the focus on the modelling approach and avoid unnecessary analytical detail, the discussion in this work refers only to the principal force contributions associated with each case, omitting specific equations and numerical parameters. In this classification, cases S03 through PR10 pertain to static loading, while the remaining configurations are intended for assessing the frame's fatigue behavior under repeated service conditions.

It should be noted that Table 2 reports only the most representative load contributions, as identified through the sensitivity analysis previously carried out in [46]. The sensitivity analysis was performed following a five-step methodology aimed at understanding how variations in input data propagate through the model to identify the most significant load scenarios affecting the bogie frame's performance. The study involved testing 20 load cases across six critical nodes of the structure, where each load contribution was analyzed at 25%, 50%, 75%, and 100% of the value required by the reference standard to verify linear behavior and maintain the criticality of the considered cases. To standardize the comparison of input parameters, a dimensionless local normalized index I_{ij} was defined as the ratio between the stress at a specific node and the maximum stress recorded at that same node across all scenarios. Subsequently, a Global Index G_j was calculated as the sum of the normalized values across all critical nodes for each load case, providing a comprehensive metric to highlight the overall effect of parameter variations and isolate the most influential cases affecting the original bogie frame. This analysis was crucial in highlighting the load conditions exerting the highest mechanical demand on a railway bogie frame. Among them, PR01 emerged as the most severe, revealing the significant influence of suspended masses on stress patterns. V04, which encompasses the combined loading acting on the main support interfaces, further highlighted the structural relevance of these boundary regions. Finally, the F1 configuration, characterized by the internal pressure of the secondary suspension together with the bogie twist, proved particularly demanding when superimposed with operational loads, resulting in a critical condition for the structure. The outcomes of the sensitivity assessment provided the foundation for the subsequent stage of the work, enabling the execution of the two topology-optimization stages on the bogie frame. The results in terms of G_j are illustrated in Figure 4.

Table 2. Main load scenarios derived from sensitivity analysis.

Load Scenario	Description
S03	Lifting on 2 points positioned diagonally on the frame
S04	Main and operative loads
PR01	Main and operative loads, including main systems mass
V04	Combination of loads focused on the principal supports
V05	Exceptional load under truck twist condition
PR10	Max load on secondary suspension (three wheels constrained)
F1	Combination of main loads, operative loads, internal pressure of the air springs and truck twist
F2	Combination of main loads, operative loads, internal pressure of the air springs and truck twist (opposite sign)

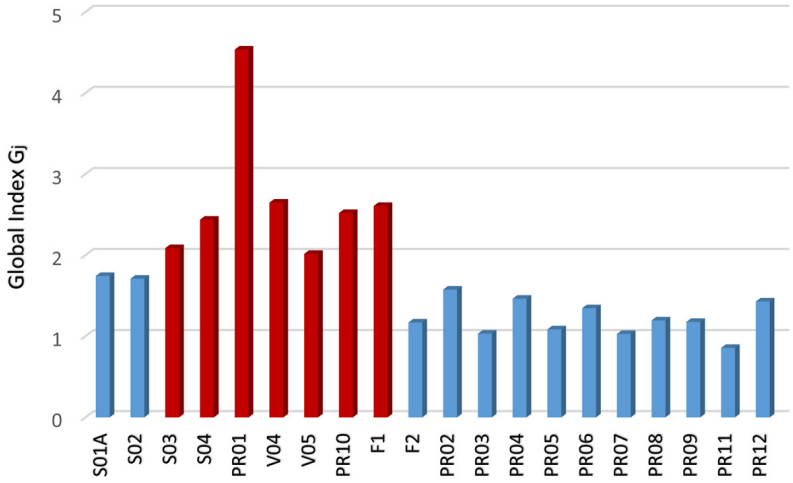

Figure 4. Results of sensitivity analysis on load scenarios [46].

3.2. Topological Optimization Result and Innovative Bogie Frame Design

In this section, the outcomes of the topology optimization process are presented, illustrating the evolution from the initial design space to the final optimized geometry. The resulting innovative bogie frame architecture is detailed, highlighting the strategic redistribution of material and the structural solutions adopted to fulfill the specific requirements of the motor bogie frame.

3.2.1. Global Optimization Results

Figure 5 presents the results of iterations ID01, ID02, and ID05, representative of the first stage of the global topology optimization. In the initial iteration, the solver was granted substantial freedom, with only the mass-fraction target imposed and no additional constraints. Although this exploratory step is often overlooked, it plays a crucial role by providing an initial visualization of the principal material distribution in response to the applied load cases. Subsequent iterations, in which additional constraints and parameters are introduced, should produce results that remain consistent with the trends observed in this preliminary assessment. The outcome of iteration ID02 confirms the overall material distribution observed in the first iteration while highlighting the effects of additional design constraints. The impact of the symmetry constraint is clearly visible on both the cross-members and the longitudinal beams, with material added in the extremities to satisfy symmetry requirements and to account for potential local stress concentrations. Since no

extraction-direction constraint was applied at this stage, the material distribution remains unrestricted in terms of manufacturability. A more pronounced change is observed in iteration ID05, where the material layout differs significantly from the previous cases. The influence of both the reduced minimum feasible feature size and the extraction-direction constraint is evident on the cross-members, which now exhibit hollowed sections with thin walls. The longitudinal beams also adopt a hollow geometry consistent with the redesigned cross-members, reflecting the combined effect of manufacturability constraints and structural efficiency considerations. These results demonstrate the progressive refinement of the topology as additional design restrictions are imposed, highlighting the solver's capability to reconcile structural performance with manufacturing feasibility while preserving the primary load paths identified in the initial exploratory iteration.

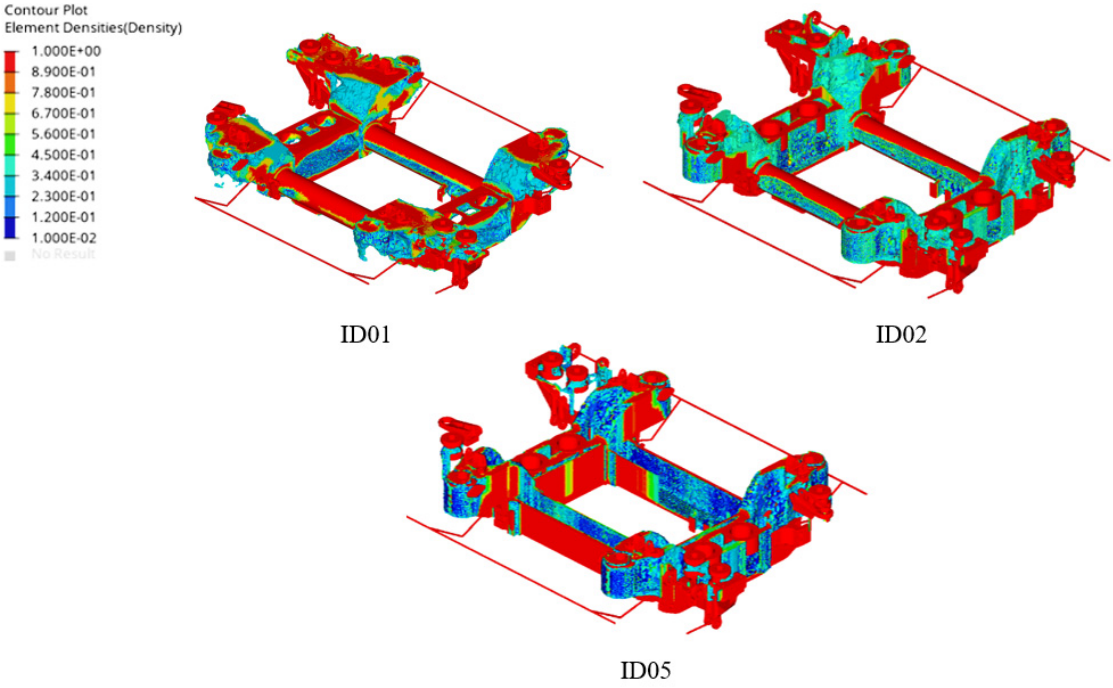

Figure 5. First global optimization stage: main results and material distributions.

Figure 6 reports the evolution of the normalized mass of the bogie frame throughout the various optimization runs. A first observation concerns the influence of the number of active parameters on the convergence behavior. When the optimization is driven by a reduced set of constraints and settings, the solver requires fewer iterations to reach an equilibrium configuration, reflecting a shorter computational time. However, this simplification inevitably limits the control over several key aspects of the redesign process, reducing the possibility to match geometries fully aligned with the targets of the research. When the remaining optimization parameters were progressively introduced, the trend of the normalized mass exhibited a more articulated evolution. In particular, the reduction of the minimum feasible feature size resulted in a significant mass decrease, approximately 18% between configurations ID02 and ID04, confirming the sensitivity of the topology to the minimum characteristic length scale allowed during the computation. A further modification concerned the tightening of the allowable stress constraint, reduced by about 20%. This adjustment produced a slight increase in the final mass. Such behavior is consistent with the requirement to reinforce localized regions where the solver detected stress peaks, thereby increasing the material content to maintain structural integrity under demanding loading conditions. Overall, the mass evolution highlights the delicate balance

between computational efficiency, constraint-driven control of the design space, and the structural robustness required by the optimization objectives.

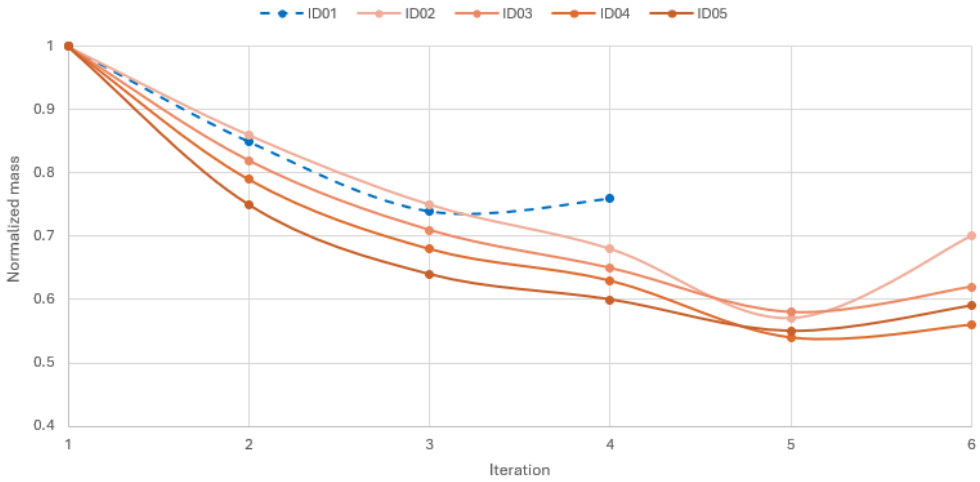

Figure 6. First global optimization stage: normalized mass function.

3.2.2. Local Optimization Results

Figure 7 illustrates the results of the local topology optimization applied to the transverse beams, corresponding to iterations ID06 and ID07. Both cross-members exhibit a similar structural behavior, although their orientation differs due to the specific loading and boundary conditions applied. In both cases, the beams adopt a hollow configuration, demonstrating the effectiveness of this type of geometry with reference to the load conditions and paths. This outcome is particularly significant, as it demonstrates that the manufacturing constraint effectively guided the solver to orient the geometry of the cross-members in a manner consistent with the underlying load paths identified during the optimizations. By preserving the structural efficiency while ensuring producibility, the resulting topology allows for substantial material reduction, offering wide-ranging possibilities for weight savings across the entire bogie frame. Furthermore, the hollow nature of the transverse beams underscores their critical role in maintaining stiffness and stability, confirming that material can be selectively removed in non-critical regions without compromising performance. This localized optimization phase complements the results of the global study, providing a more refined and targeted redesign that combines structural efficiency, manufacturing feasibility, and weight reduction, ultimately supporting the development of a lighter and more efficient tram bogie frame.

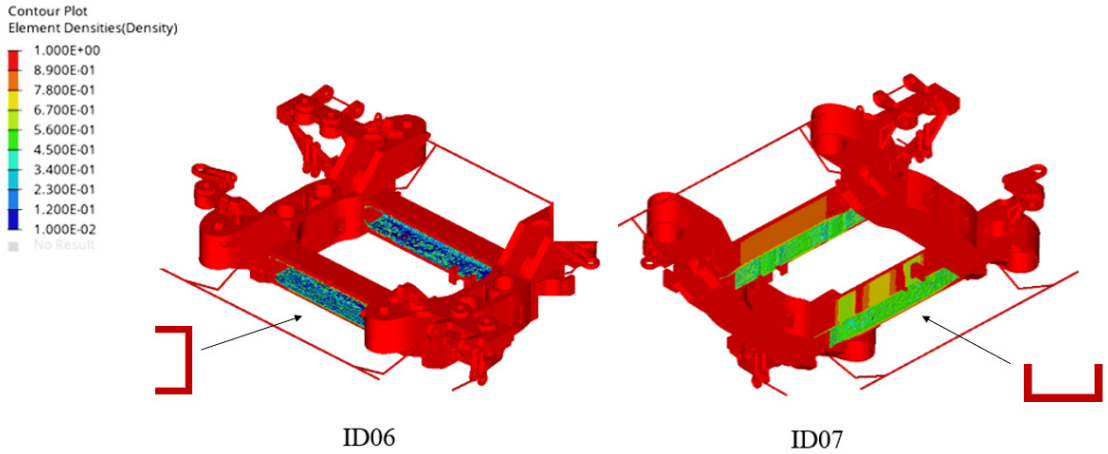

Figure 7. Second local optimization stage: main results and material distributions.

3.2.3. Railway Motor Bogie Frame: Innovative Design

In the final stage of the study, attention was devoted to translating the optimized topology of the motor bogie frame into a geometry suitable for engineering use and compliant with industrial manufacturing requirements. Although the topology optimization procedure effectively highlights the most efficient material layout for meeting the structural targets, its output typically consists of irregular and fragmented shapes that cannot be directly produced using standard fabrication processes, as shown in Figure 8. For this reason, a dedicated redesign phase was carried out to convert the optimized structural concept into a coherent and manufacturable frame architecture. This reconstruction step required the integration of engineering judgement to smooth discontinuities, regularize surface transitions, and remove thin or isolated features that are incompatible with practical production constraints. Particular care was taken to preserve the main load paths identified during the optimization campaign, ensuring that the redesigned frame maintains the stiffness and strength benefits revealed by the numerical results. Where geometric simplifications were necessary, a controlled amount of material was reintroduced to guarantee structural soundness while retaining the weight reduction achieved through optimization. The resulting geometry therefore represents a balanced compromise between numerical optimality and industrial feasibility, ensuring compatibility with typical casting-manufactured components, and preserving the functional interfaces required for integration within the motor bogie assembly.

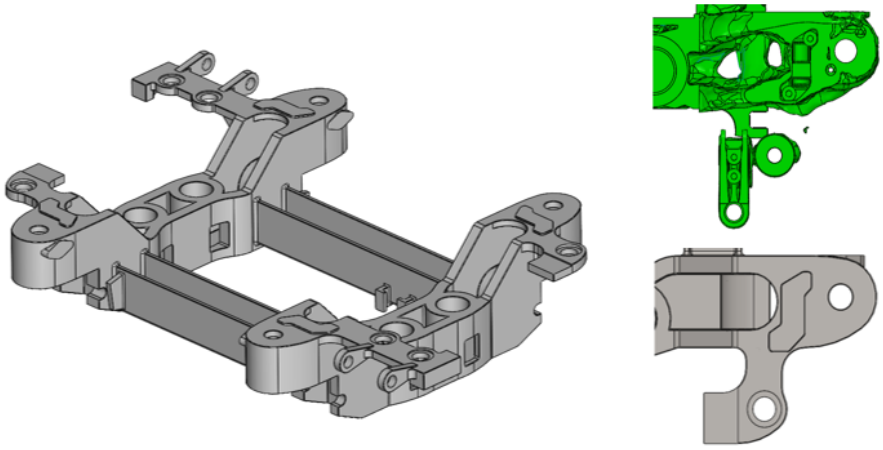

Figure 8. New design of motor bogie frame (CAD view and irregular surface re-building).

Once the reconstructed geometry of the optimized frame was defined, the component was re-imported into the finite element environment to generate a new discretization. This step is essential because the morphology of the reconstructed model could differ significantly from the raw topology produced by the optimization algorithm, requiring an updated mesh capable of accurately capturing the new surfaces, fillets, and thickness variations introduced during the geometric reconstruction phase. At this stage, the correct definition of the design space, particularly the explicit isolation of all interfaces with the various connected components, becomes crucial. A properly structured design space ensures that the FE model can be updated rapidly and consistently, while minimizing the risk of human-induced errors during geometry cleaning and mesh regeneration.

3.3. Structural Performance Assessment

The optimized bogie frame was subsequently evaluated under the seven prescribed load scenarios defined by the reference standard. For each condition, a structural assessment was carried out by examining the stress response at all nodes of the finite element

discretization. Before performing the full set of simulations, a mesh-sensitivity analysis was conducted, taking into account both the outcomes of the topology optimization and the minimum feasible feature dimension introduced during the reconstruction phase. An initial element size of 20 mm was progressively reduced down to 12 mm in order to assess the influence of mesh refinement on the predicted maximum stress. The results showed that, starting from an element size of approximately 15 mm, the variation in maximum stress stabilized within a 3–4% margin. This behavior confirmed that further refinement would not significantly improve accuracy, allowing the selection of a mesh density that provides an optimal balance between computational cost and result reliability. Figure 9 presents the static analysis results obtained for the optimized bogie frame, where stress values have been normalized to improve readability. The maximum stress recorded is approximately 600 MPa, which represents a relatively high value with reference to traditional construction steels used for bogie frames. However, as illustrated in the figure, the peak stresses remain highly localized at the extremities of the redesigned crossbeam, in a manner consistent with the behavior of the original configuration. A potential refinement strategy would involve a detailed redesign of this region, introducing larger fillet radii to mitigate local stress-intensity factors, followed by a dedicated nonlinear sub-modeling analysis to evaluate potential material plasticization. These activities, however, pertain to an advanced design-for-manufacturing stage and fall outside the scope of the present research. The figure also compares two alternative frame configurations obtained during the optimization workflow, characterized by a 90° rotation of the crossbeam opening with respect to one another. The resulting stress distributions demonstrate a high degree of consistency, with peak values that are essentially comparable across the two layouts, further confirming the robustness of the reconstructed geometry.

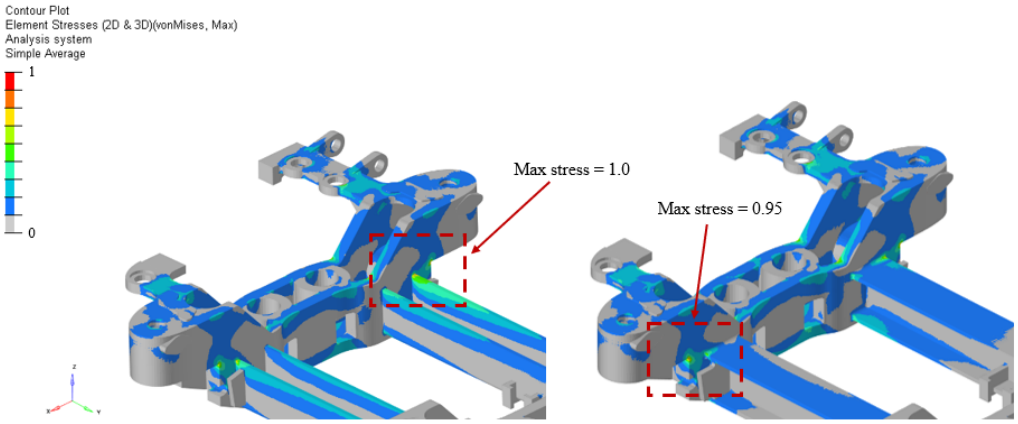

Figure 9. Normalized static stress distribution for two different configurations of the new design of the bogie frame.

With regard to the fatigue performance assessment, Figure 10 presents the distribution of the maximum absolute principal stress for the two frame configurations. This stress component represents the reference quantity for conducting the multiaxial fatigue analysis, as it enables an accurate estimation of the stress range $\Delta\sigma$ to be compared with the material S–N curves. The post-processing stage for fatigue evaluation is strongly dependent on the selected reference standard, which provides the criteria for interpreting stress amplitudes, mean-stress corrections, and damage accumulation rules. In this context, particular attention must be paid to the comparison between the computed stress range and the corresponding characteristic curve of the material in order to obtain a reliable estimation of the local fatigue damage. The two frame configurations exhibit comparable distributions of the maximum principal stress, confirming the consistency of the structural response and

the robustness of the optimized design with respect to fatigue-critical load conditions. It is important to note that the visualization scale is again normalized between +1 and −1, since in a purely compressive state the maximum principal stress may assume negative values. The zero level is intentionally not placed at the midpoint of the scale, in order to allocate greater resolution to the tensile stress range, which is the most critical aspect for fatigue assessment. The resulting stress magnitudes are generally low across the entire structure, with only a few localized peaks that may require a dedicated, higher-fidelity refinement in a subsequent development phase of the frame. Such future work would include a more detailed geometric definition of the affected zones and a more accurate fatigue evaluation to quantify the local damage potential.

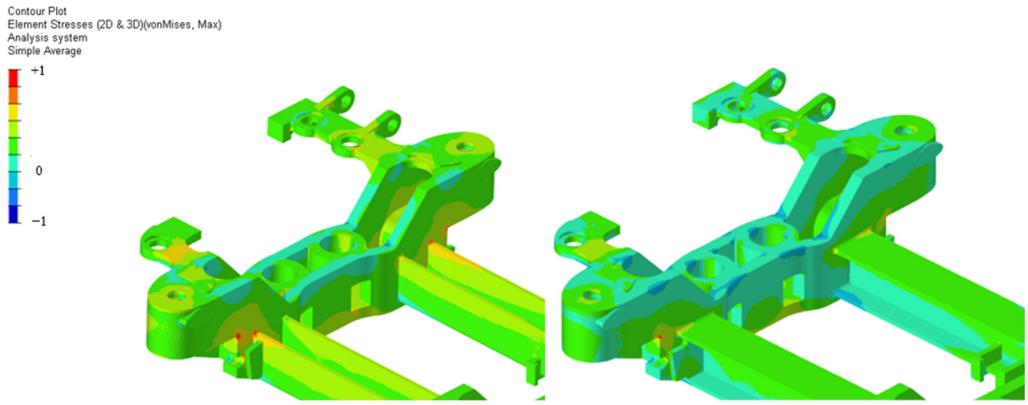

Figure 10. Normalized maximum absolute principal stress distribution for two different configurations of the new design of the bogie frame.

Table 3 reports a comparison of the first five flexible modes obtained for the original bogie frame and for the optimized configuration featuring the rotated cross-beam opening. The first vibration mode shown in Figure 11, which already lies above 60 Hz, is characterized by a highly localized deformation pattern concentrated at the frame extremities, particularly in the region of the traction support, as expected for a motor bogie frame. Both the first eigenvalue, which exhibits a variation of approximately 1%, and the corresponding eigenvector, which retains its predominantly bending-dominated shape, demonstrate a strong consistency with the baseline configuration. This result is of primary importance, as it confirms that the redesigned frame preserves not only all mechanical interfaces with the surrounding subsystems but also its fundamental dynamic behavior. Such preservation ensures compatibility with the existing vehicle architecture (thanks to the non-design space definition) and facilitates a seamless replacement of the original frame with the optimized one, minimizing integration effort and reducing the need for downstream redesign.

Table 3. Modal analysis results and comparison.

Mode Number	Original Design [Hz]	Optimized Design [Hz]	Δ %
1	63.66	64.63	+1.0
2	101.85	134.64	+32.0
3	115.28	138.05	+19.8
4	201.57	197.63	−2.0
5	247.50	224.87	−9.1

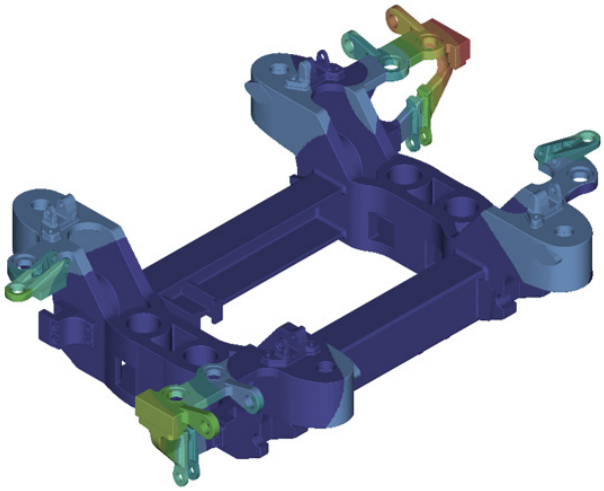

Figure 11. Mode shape 1 for the new design of the bogie frame: flexural mode localized on the traction equipment support.

4. Conclusions and Future Developments

This research activity focused on the structural redesign and performance assessment of a railway motor bogie frame through a comprehensive topology-optimization-based methodology, fully compliant with the European reference standard governing the design of such complex components. The study relied on an extensive numerical simulation campaign aimed at evaluating the influence of key optimization parameters and identifying the most effective configuration capable of delivering an innovative yet feasible bogie frame design through a fast, efficient, and reliable workflow. This process was further supported by a detailed sensitivity analysis performed to determine the most critical load scenarios in terms of structural resistance. The proposed optimization strategy adopted a two-stage approach. In the first, global optimization stage, the structural performance of the entire bogie frame was evaluated, showing the main load paths and revealing how the introduction of multiple design parameters can increase the number of solver iterations by approximately 50%, thereby affecting computational time, although not in a strictly proportional manner. Symmetry constraints proved to be particularly effective, both in terms of improving the clarity of the optimized topology and in simplifying the subsequent geometry reconstruction phase. Among all parameters investigated, the minimum feasible feature dimension had the strongest impact on the final optimized solution, producing significant changes in both material distribution and overall mass. A maximum mass reduction of approximately 18% was observed while preserving the required stiffness and strength pathways. The second, more localized optimization stage, focused on the crossbeams, highlighted the importance of manufacturing constraints, which introduced additional flexibility in managing the solver while ensuring the feasibility of the final design. The static and fatigue assessment did not aim merely at quantifying utilization factors but rather at verifying that the stress distribution remained consistent with that of the original frame. This approach allows designers to more effectively evaluate whether the innovative structure could benefit from alternative, higher-performance materials based on the observed stress patterns. All optimized configurations demonstrated coherent and physically reasonable stress distributions, confirming the robustness of the proposed methodology. Finally, the dynamic analysis showed that the redesigned bogie frame retained modal characteristics highly consistent with the original configuration. The first flexible mode appears at a frequency higher than 60 Hz, with the first eigenvalue showing a variation of only about 1% compared with the baseline design. Moreover, the first eigenvector preserves its flexural nature and remains localized mainly at the frame

extremities and in the traction-support region, exactly as in the original design. These results are of primary importance: by maintaining both the interface geometry and the dynamic behavior of the bogie frame, the innovative configuration can be seamlessly integrated into the existing bogie system, enabling rapid replacement of the conventional frame without requiring modifications to surrounding subsystems. Overall, the study demonstrates that a carefully structured topology-optimization workflow, supported by systematic sensitivity analyses and followed by rigorous static, fatigue, and dynamic verification, can lead to a manufacturable, structurally efficient, and dynamically compatible innovative bogie frame design. This confirms the suitability and robustness of the proposed methodology for future developments in railway bogie structural optimization.

Author Contributions: Conceptualization, methodology, software, simulation, validation, review A.C.; review, supervision, project administration E.M. and A.R. All authors have read and agreed to the published version of the manuscript.

Funding: This study was supported by MOST Sustainable Mobility National Research Center and received funding from the European Union Next GenerationEU (PIANO NAZIONALE DI RIPRESA E RESILIENZA (PNRR) MISSIONE 4 COMPONENTE 2, INVESTIMENTO 1.4 D.D. 1033 17/06/2022, CN00000023).

Institutional Review Board Statement: Not applicable.

Informed Consent Statement: Not applicable.

Data Availability Statement: The original contributions presented in this study are included in the article. Further inquiries can be directed to the corresponding author.

Conflicts of Interest: The authors declare no conflicts of interest.

References

1. Kong, Y.; Abdullah, S.; Omar, M.; Haris, S. Topological and Topographical Optimization of Automotive Spring Lower Seat. *Lat. Am. J. Solids Struct.* **2016**, *13*, 1388–1405. [CrossRef]
2. Jankovics, D.; Barari, A. Customization of Automotive Structural Components using Additive Manufacturing and Topology Optimization. *IFAC-PapersOnLine* **2019**, *52*, 212–217. [CrossRef]
3. Su, H.; An, D.; Ma, L.; He, Y. A survey of multi-scale optimization methods in fiber-reinforced polymer composites design for automobile applications. *Proc. Inst. Mech. Eng. Part D J. Automob. Eng.* **2024**, 09544070251327706. [CrossRef]
4. Billur, S.; Raju, G.U. Mass Optimization of Automotive Radial Arm Using FEA for Modal and Static structural Analysis. *IOP Conf. Ser. Mater. Sci. Eng.* **2021**, *1116*, 012113. [CrossRef]
5. Viqaruddin, M.; Reddy, D.R. Structural optimization of control arm for weight reduction and improved performance. *Mater. Today Proc.* **2017**, *4*, 9230–9236. [CrossRef]
6. Matsimbi, M.; Nziu, P.K.; Masu, L.M.; Maringa, M. Topology optimization of automotive body structures: A review. *Int. J. Eng. Res. Technol.* **2021**, *13*, 4282–4296.
7. Yan, L.; Guo, Q.; Yang, S.; Liao, X.; Qi, C. A size optimization procedure for irregularly spaced spot weld design of automotive structures. *Thin-Walled Struct.* **2021**, *166*, 108015. [CrossRef]
8. Yang, S.; Yan, L.; Qi, C. An adaptive multi-step varying-domain topology optimization method for spot weld design of automotive structures. *Struct. Multidiscip. Optim.* **2018**, *59*, 291–310. [CrossRef]
9. Liu, Y.; Liu, Z.; Qin, H.; Zhong, H.; Lv, C. An efficient structural optimization approach for the modular automotive body conceptual design. *Struct. Multidiscip. Optim.* **2018**, *58*, 1275–1289. [CrossRef]
10. Fonseca, J.; Lee, J.; Jang, W.; Han, D.; Kim, N.; Lee, H. Manufacturability-constrained optimization for enhancing quality and suitability of injection-molded short fiber-reinforced plastic/metal hybrid automotive structures. *Struct. Multidiscip. Optim.* **2023**, *66*, 113. [CrossRef]
11. Zhu, J.; Zhou, H.; Wang, C.; Zhou, L.; Yuan, S.; Zhang, W. A review of topology optimization for additive manufacturing: Status and challenges. *Chin. J. Aeronaut.* **2020**, *34*, 91–110. [CrossRef]
12. Zegard, T.; Paulino, G. Bridging topology optimization and additive manufacturing. *Struct. Multidiscip. Optim.* **2016**, *53*, 175–192. [CrossRef]

13. Wang, W.; Munro, D.; Wang, C.; van Keulen, F.; Wu, J. Space-time topology optimization for additive manufacturing. *Struct. Multidiscip. Optim.* **2019**, *61*, 1–18. [CrossRef]
14. Sabiston, G.; Kim, I. 3D topology optimization for cost and time minimization in additive manufacturing. *Struct. Multidiscip. Optim.* **2020**, *61*, 731–748. [CrossRef]
15. Bandini, A.; Cascino, A.; Meli, E.; Pinelli, L.; Marconcini, M. Improving Aeromechanical Performance of Compressor Rotor Blisk with Topology Optimization. *Energies* **2024**, *17*, 1883. [CrossRef]
16. Cascino, A.; Meli, E.; Rindi, A.; Pucci, E.; Matoni, E. Experimental Validation and Dynamic Analysis of Additive Manufacturing Burner for Gas Turbine Applications. *Machines* **2025**, *13*, 1111. [CrossRef]
17. Pietropaoli, M.; Ahlfeld, R.; Montomoli, F.; Ciani, A.; D'eRcole, M. Design for Additive Manufacturing: Internal Channel Optimization. In Proceedings of the ASME Turbo Expo 2016: Turbomachinery Technical Conference and Exposition, Seoul, Republic of Korea, 13–17 June 2016; ASME: New York, NY, USA, 2016; Volume 5B: Heat Transfer, p. V05BT11A013.
18. Srivastava, P.K.; Shukla, S. Topology Optimization: Weight Reduction of Indian Railway Freight Bogie Side Frame. *Int. J. Mech. Eng.* **2021**, *6*, 4374–4383.
19. Yamamoto, M. Non-parametric optimization of railway wheel web shape based on fatigue design criteria. *Int. J. Fatigue* **2020**, *134*, 105463. [CrossRef]
20. Cascino, A.; Meli, E.; Rindi, A. Development of a Design Procedure Combining Topological Optimization and a Multibody Environment: Application to a Tram Motor Bogie Frame. *Vehicles* **2024**, *6*, 1843–1856. [CrossRef]
21. Gersborg, A.R.; Andreasen, C.S. An explicit parameterization for casting constraints in gradient driven topology optimization. *Struct. Multidiscip. Optim.* **2011**, *44*, 875–881. [CrossRef]
22. Cascino, A.; Meli, E.; Rindi, A. Development of a Methodology for Railway Bolster Beam Design Enhancement Using Topological Optimization and Manufacturing Constraints. *Eng* **2024**, *5*, 1485–1498. [CrossRef]
23. Cascino, A.; Meli, E.; Rindi, A. Lightweight Design and Topology Optimization of a Railway Motor Support Under Manufacturing and Adaptive Stress Constraints. *Vehicles* **2026**, *8*, 3. [CrossRef]
24. Lang, D.; Radford, D.W. Design Optimization of a Composite Rail Vehicle Anchor Bracket. *Urban Rail Transit* **2021**, *7*, 84–100. [CrossRef]
25. Xiu, R.; Spiryagin, M.; Wu, Q.; Yang, S.; Liu, Y. Fatigue life prediction for locomotive bogie frames using virtual prototype technique. *Proc. Inst. Mech. Eng. Part F J. Rail Rapid Transit* **2021**, *235*, 1122–1131. [CrossRef]
26. Guo, F.; Wu, S.C.; Liu, J.X.; Zhang, W.; Qin, Q.B.; Yao, Y. Fatigue life assessment of bogie frames in high-speed railway vehicles considering gear meshing. *Int. J. Fatigue* **2020**, *132*, 105353. [CrossRef]
27. Luo, R.K.; Gabbitas, B.L.; Brickle, B.V. Fatigue Life Evaluation of a Railway Vehicle Bogie Using an Integrated Dynamic Simulation. *Proc. Inst. Mech. Eng. Part F J. Rail Rapid Transit* **1994**, *208*, 123–132. [CrossRef]
28. Luo, R.; Gabbitas, B.; Brickle, B. Dynamic stress analysis of an open-shaped railway bogie frame. *Eng. Fail. Anal.* **1996**, *3*, 53–64. [CrossRef]
29. Mi, C.; Li, W.; Xiao, X.; Jian, H.; Gu, Z.; Berto, F. Lifetime assessment and optimization of a welded a-type frame in a mining truck considering uncertainties of material properties and structural geometry and load. *Appl. Sci.* **2019**, *9*, 918. [CrossRef]
30. Zhou, W.; Zhang, G.; Wang, H.; Peng, C.; Liu, X.; Xiao, H.; Liang, X. Experimental fatigue evaluation of bogie frames on metro trains. *Machines* **2022**, *10*, 1003. [CrossRef]
31. Wang, W.; Bai, J.; Wu, S.; Zheng, J.; Zhou, P. Experimental investigations on the effects of fatigue crack in urban metro welded bogie frame. *Appl. Sci.* **2020**, *10*, 1537. [CrossRef]
32. Kirsch, K.L.; Thole, K.A. Experimental Investigation of Numerically Optimized Wavy Microchannels Created Through Additive Manufacturing. *J. Turbomach.* **2018**, *140*, 021002. [CrossRef]
33. Cho, J.G.; Koo, J.S.; Jung, H.S. A lightweight design approach for an EMU carbody using a material selection method and size optimization. *J. Mech. Sci. Technol.* **2016**, *30*, 673–681. [CrossRef]
34. Koenig, J. Integral consideration of the lightweight design for railway vehicles. In *Young Researchers Seminar*; Technical University of Denmark: Kongens Lyngby, Denmark, 2011.
35. Cascino, A.; Meli, E.; Rindi, A. High-Fidelity Finite Element Modelling (FEM) and Dynamic Analysis of a Hybrid Aluminium–Honeycomb Railway Vehicle Carbody. *Appl. Sci.* **2026**, *16*, 549. [CrossRef]
36. Cascino, A.; Meli, E.; Rindi, A. Design and Optimization of a Hybrid Railcar Structure with Multilayer Composite Panels. *Materials* **2025**, *18*, 5013. [CrossRef]
37. Miao, B.; Luo, Y.; Peng, Q.; Qiu, Y.; Chen, H.; Yang, Z. Multidisciplinary design optimization of lightweight carbody for fatigue assessment. *Mater. Des.* **2020**, *194*, 108910. [CrossRef]
38. *EN 12663-1:2015*; Railway Applications—Structural Requirements of Railway Vehicle Bodies—Part 1: Locomotives and Passenger Rolling Stock (and Alternative Method for Freight Wagons). German Institute for Standardisation: Berlin, Germany, 2015.
39. *UNI EN 15663:2019*; Railway Applications—Vehicle Reference Masses. UNI (Ente Nazionale Italiano di Unificazione): Milan, Italy, 2019.

40. Kumar, W.; Sharma, U.K.; Shome, M. Mechanical properties of conventional structural steel and fire-resistant steel at elevated temperatures. *J. Constr. Steel Res.* **2021**, *181*, 106615. [CrossRef]
41. Jameson, A. *Gradient Based Optimization Methods*; MAE Technical Report No. 2057; Princeton University: Princeton, NJ, USA, 1995.
42. Bruggi, M.; Duysinx, P. Topology optimization for minimum weight with compliance and stress constraints. *Struct. Multidiscip. Optim.* **2012**, *46*, 369–384. [CrossRef]
43. Liu, K.; Yeoh, K.; Cui, Y.; Zhao, A.; Luo, Y.; Zhong, Z. Integrated multiscale topology optimization of frame structures for minimizing compliance. *Eng. Struct.* **2025**, *339*, 120561. [CrossRef]
44. Dunning, P.; Kim, H. Robust Topology Optimization: Minimization of Expected and Variance of Compliance. *AIAA J.* **2013**, *51*, 2656–2664. [CrossRef]
45. *EN 13749:2021*; Railway Applications—Wheelsets and Bogies—Method of Specifying the Structural Requirements of Bogie Frames. The European Committee for Standardization (CEN): Brussels, Belgium, 2021.
46. Cascino, A.; Meli, E.; Rindi, A. A New Strategy for Railway Bogie Frame Designing Combining Structural–Topological Optimization and Sensitivity Analysis. *Vehicles* **2024**, *6*, 651–665. [CrossRef]